BEAM SIZE MEASUREMENTS USING SYNCHROTRON RADIATION INTERFEROMETRY AT ALBA

L. Torino, U. Iriso, ALBA-CELLS, Cerdanyola, Spain
T. Mitsuhashi, KEK, Tsukuba, Japan

Abstract

First tests to measure the transverse beam size using interferometry at ALBA showed that the measurement reliability was limited by the inhomogeneous light wavefront arriving at the double slit system. For this reason, the optical components guiding the synchrotron radiation have been exchanged, and detailed quality checks have been carried out using techniques like the Fizeau interferometry or Hartmann mask tests. We report the results of the analysis of the optical elements installed in the beamline, and the beam size measurements performed using double slit interferometry in both horizontal and vertical planes.

INTRODUCTION

ALBA is a 3 GeV third generation synchrotron light source operative for users since 2012 [1].

Due to the machine small emittance it is not possible to measure the beam size by using a simple imaging system because of the diffraction limit. Measurements of the beam size are nowadays routinely performed using a x-ray pinhole camera [2]. In order to have a second reliable measurement of this parameter the double slit synchrotron radiation interferometry technique (SR interferometer) [3] has been proposed and is still under development. Preliminary tests were performed at the diagnostic beamline Xanadu using the already existing optical components which quality was not good enough to provide the best results [4].

In this report we describe the improvement of the beamline optical components and the tests performed to ensure their quality. We also report some results of the interferometry measurements.

THE SR INTERFEROMETER

The main parameters of the ALBA lattice that determine the transverse beam size at the source point are listed in Table 1.

Table 1: ALBA Lattice Parameters

	x	y
β	0.299 m	25.08 m
Dispersion	0.04 m	0 m
Energy spread	0.001 01	—
Emittance	4.6 nm	0.023 nm
Beam size	53.6 µm	23.9 µm

One of the most common techniques to measure beam sizes in this range is the SR interferometer. Using a double slit interferometer the degree of spatial coherence of the synchrotron radiation produced by the beam is measured, from where the beam size can be inferred. A sketch is presented in Fig. 1.

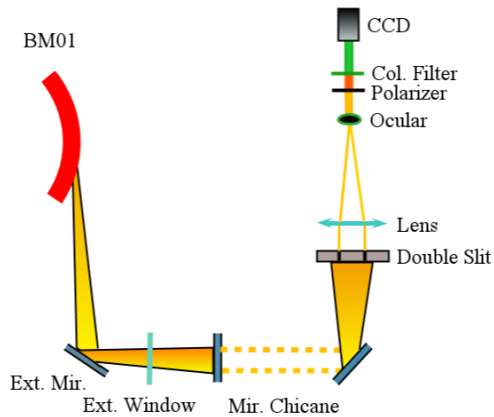

Figure 1: Sketch of the SR interferometer setup at ALBA. The optical path is composed by 6 mirrors in atmospheric pressure. The extraction mirror is set in the vacuum.

The visible part of the radiation produced by the electron beam passing through a bending magnet (BM01) is extracted by an in-vacuum mirror located at 8.635 m from the source and at $\simeq$ 6 mm from the beam orbit plane. In this way the extraction mirror is not in contact with hard x-rays that may compromise its characteristics. Only the radiation produced with a positive angle with respect to the beam orbit plane is collected, for this reason the mirror is said to be an "half-mirror". The light is extracted through a window and guided out from the tunnel up to the optical table in the beamline by 6 mirrors. The interferometer system is composed by a double slit aperture that produces the interferogram. The width of the slits is 1 mm and the height is chosen depending on the quantity of light needed. The separation between the two slits is variable from 8 mm to 22 mm. Immediately after the double slit an apochromat (BORG ED500) lens with focal length of 500 mm and flatness $\frac{\lambda}{10}$ is located. After the focal point an ocular (Takahashi MC LE 18 mm) is introduced to magnify the image. A polarizer and a 540 nm narrow bandpass color filter (width 10 nm) both from Thorlabs are used to select the σ radiation polarization and energy. Finally the interferogram is captured by a CCD camera whose pixel size is 3.75 µm × 3.75 µm.

WAVEFRONT ERROR

In order to obtain good measurements the wavefront error due to the quality of the optical components has to be

ISBN 978-3-95450-141-0

minimized. Previous measurements showed that optical components of Xanadu were not suitable to obtain good measurements [4]. For this reason the extraction mirror, the extraction window and all the mirrors of the optical path were changed. The quality of each component was tested before the installation.

In particular the most critical component of the diagnostic beamline is the extraction mirror. This mirror is located in-vacuum and is designed for ultra-high vacuum and high temperature (bake-outing at 80 °C). To prevent the deformation due to over heating the mirror is provided with thermocouples that measure directly the temperature at its bottom. A motorized system allows to move the mirror vertically in and out from the radiation fan, down to 5 mm from the orbit plane. The routine position is set to 6 mm.

Old Xanadu Beamline

Xanadu beamline was not meant to perform precise optical measurements such as interferometry. The mirrors used before the beamline upgrade to bring the light to the optical table were aluminum with 2" diameter from Thorlabs. They were small with respect to the radiation fan and cut the radiation at the border.

The extraction mirror was made of copper and with a designed flatness of $\frac{\lambda}{2}$. The mirror had not been measured before the use, but it was clear that the wavefront reaching the beamline was strongly deformed. To measure the wavefront deformation caused by all the transport line a Hartmann mask was used.

The Hartmann mask is a thin plate over which little holes are present (Fig. 2). In particular the one used for this measurements has a matrix of (10×10) holes of 1 mm diameter spaced by 5 mm directly irradiated by synchrotron radiation. Generally the mask is used to find the focal position of optical system (specially in astronomy) but can also be used to reconstruct a wavefront after the propagation through the optical components of the transport line by converting the complex wavefront in light rays . The wavefront error is obtained by averaging the difference between the positions of the centroid of the rays after the propagation, and the position obtained considering only the wavefront (without optical components). Details on the calculations ant the theory can be found in [5]. The result for the wavefront reconstruction when using the old Xanadu mirror is shown in the first picture of Fig. 3 and the result of the calculation provides a wavefront error of $\frac{\lambda}{3}$.

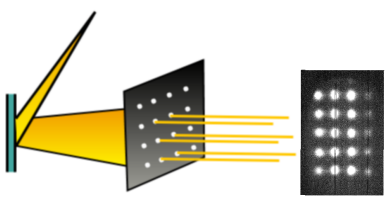

Figure 2: Sketch of the Hartmann mask working principle and a real data acquisition.

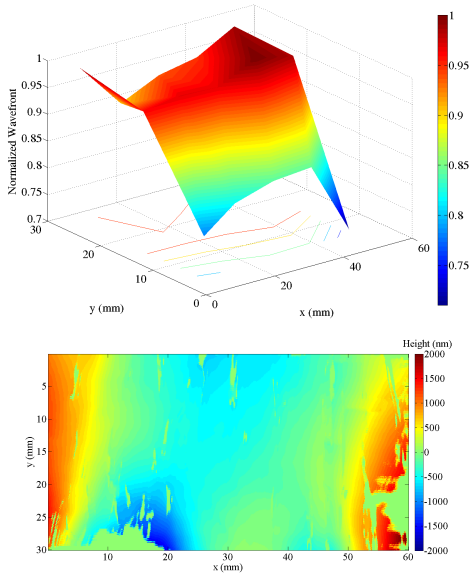

Figure 3: Wavefront reconstruction and Fizeau analysis for the old Xanadu extraction mirror.

Direct measurements of the extraction mirror flatness were performed in the ALBA optical laboratory using a Fizeau interferometer (second picture in Fig. 3). The flatness over all the mirror is around λ. Note that the flatness of the whole mirror may introduce a wavefront error worst with respect the one measured with the Hartmann mask. This is because the second measure is an approximation, and also because in this case a smaller region of the mirror is considered: the one intercepted by visible light.

It is worth mentioning that after the extraction of the old mirror the presence of some scratches compatible with a crystalline growth were evident. Moreover clear structures were visible at bare eye in the vertical direction. Further analysis shows actually that the growth is compatible with nano-crystalline diamond (see **APPENDIX**).

New Xanadu Beamline

First, all the transport mirrors were substituted by 4" mirrors always by Thorlabs with a designed flatness of $\frac{\lambda}{10}$. Also the extraction window was manufactured specially for ALBA by Torr Scientific and its flatness measured with the Fizeau interferometer was found to be $\frac{\lambda}{20}$ in the region of interest. Due care was taken to obtain a parallelism better than 5 arcsec (< 3 arcsec measured).

The new extraction mirror was produced by Thales-SESO: it is again made out of copper with a nickel coating called “kanigen” aided to protect the Cu from oxidation. The requested flatness was $\frac{\lambda}{10}$ and the 3 thermocouples feedback system to prevent overheating is also present. After the mounting on the actual mechanical support, the mirror was measured with the Fizeau interferometer and the obtained flatness is $\frac{\lambda}{7}$. Results are presented in the first picture of Fig. 4.

ISBN 978-3-95450-141-0

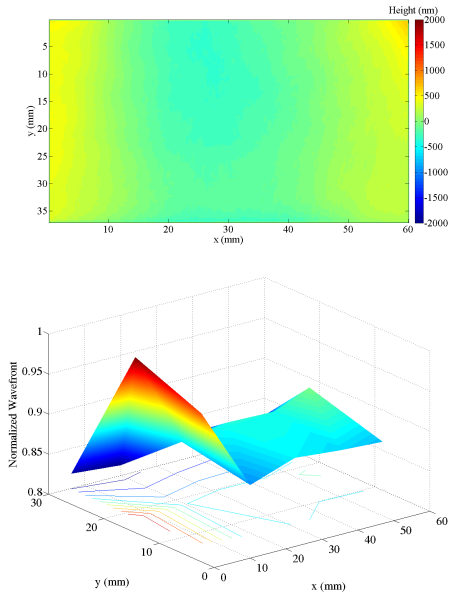

Figure 4: Fizeau analysis and wavefront reconstruction of the new extraction mirror. The color scale is the same as in Fig. 3.

The mirror appears a bit deformed on the sides because of the design of the mechanical holder, for this reason it is important to point out that the measurement were performed with the mirror mounted, in this way it is possible to directly compare the Fizeau results with the one obtained from the Hartmann mask. The wavefront deformation caused by the whole transport line, measured with the Hartmann mask is presented in the second picture of Fig. 4. The wavefront is much flatter than the one from the old mirror presented in Fig. 3 and provides an approximate wavefront error of $\frac{\lambda}{8}$.

A simple test of the good quality of the transport line can be performed using the synchrotron radiation and a three holes mask to check whether, using a focusing lens, the three rays collapse in a single spot at the focal position. The progression to find the lens focal point is shown in Fig. 5 and shows a very good quality for the transport line.

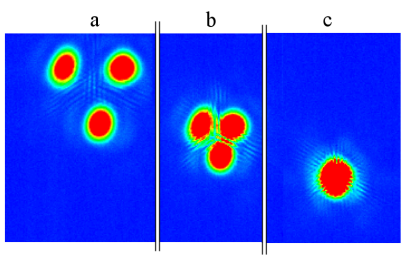

Figure 5: Test performed with a three holes mask to check the quality of the transport line. The rays produced collapse in a single spot at the focal point showing a good quality of the optical components.

In summary, the analysis of the optical components shows that the flatness of the whole mirror, measured with the Fizeau interferometer, is improved from $\frac{\lambda}{1}$ to $\frac{\lambda}{7}$ and that the total wavefront error, measured with the Hartmann mask, from $\frac{\lambda}{3}$ to $\frac{\lambda}{8}$.

BEAM SIZE MEASUREMENTS

After the upgrade of the Xanadu beamline beam size measurements were performed. The apparatus was already described in the previous sections, a typical interferogram with a slit separation of 16 mm is presented in Fig. 6.

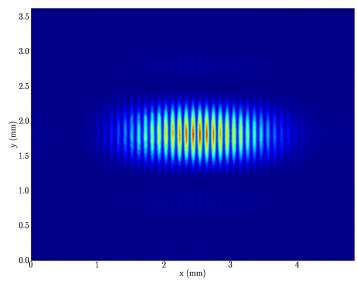

Figure 6: Typical interferogram obtained using the setup described in the first section.

The cross section of the interferogram is described theoretically by:

$$I = I_0 \left\{ \mathrm{sinc}\left(\frac{2\pi a x}{\lambda f}\right)\right\}^2 \times \left\{1 + V\cos\left(\frac{2\pi D x}{\lambda f}\right)\right\} \quad (1)$$

where I_0 is the sum of the intensity of the radiation coming from the two slits, a is the half width of the slit aperture, f is the distance between the double slits and the interference plane, D is the slit separation and V is the absolute value of the complex degree of spatial coherence (visibility). Equation 1 is used to fit the cross section of the interferogram. The theoretical equation dos not foresee the use of the ocular, for this reason the parameter related with the image magnification, f, is let as a free parameter in the fit. The same happens with I_0 since it is not possible obtain the value in advance. The other free parameter is the visibility V and extracting it from the fit it is possible to compute the beam size:

$$\sigma = \frac{\lambda L}{\pi D}\sqrt{\frac{1}{2}\ln\frac{1}{V}} \quad (2)$$

where L is the distance between the source and the double slits. Figure 7 shows an example of the fit result.

Horizontal Beam Size

Several data were taken with different slits separations. For each slit separation D several data acquisitions were taken to study the fluctuation of the result. First results showed that the measurement was not stable. Beam size result for different slit separation D are the green dots in Fig. 8, the value on the plot was calculated averaging over several

ISBN 978-3-95450-141-0

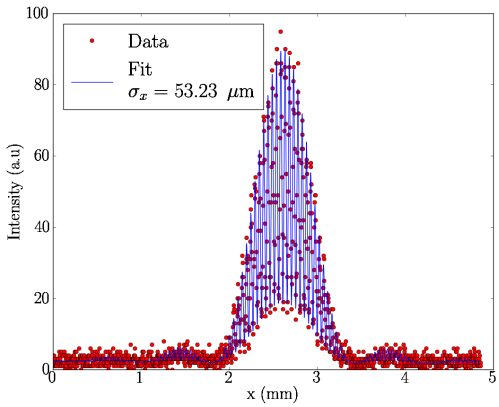

Figure 7: Fit of the cross section of the interferogram showed in Fig. 6. The expected result for the horizontal beam size is 53.6 µm as reported in Tab. 1

acquisitions and the error bar considering the standard deviation from the average. The cause of this error in the beam

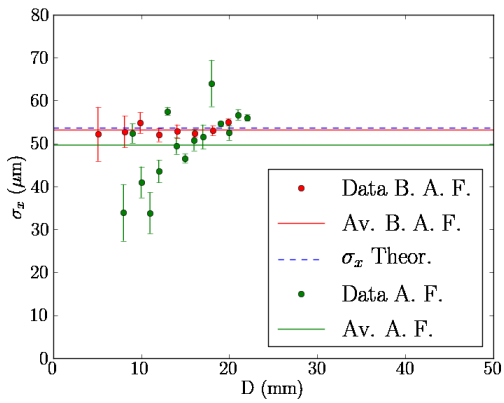

Figure 8: Horizontal beam size as a function of the slit separation blocking the air flux (red dots, average beam size 53.1 µm) and without (green dots, average 49.6 µm).

size was mainly caused by the vibration in the optical path. In particular these vibrations may be caused by air flowing between the tunnel and the Xanadu beamline through the hole driven in the shielding wall, probably due to a pressure gradient. Two neutral density filters were used to block the air flux between the tunnel and the beamline. Using this setup, measurements are more stable.

An example of the 100 data acquisitions for the horizontal beam size measurement with $D = 16$ mm is shown in Fig. 9. The final beam size average on a value that is very close to the expected one. Again the measurement was repeated for different slit separations. The results are presented in red dots in Fig. 8. for all the D the beam size result is compatible with the expected one, which indicates a Gaussian beam profile.

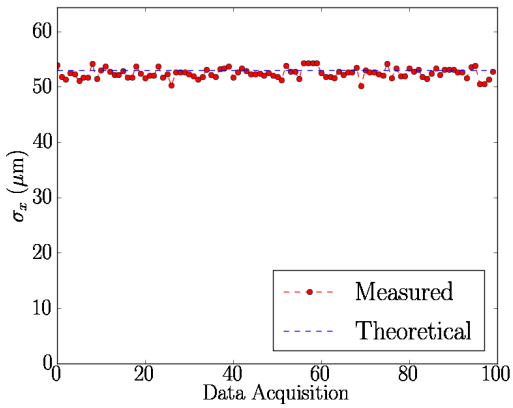

Figure 9: Trend of the fitted horizontal beam size for 100 acquisitions.

Vertical Beam Size

Synchrotron radiation is not homogeneous vertically and moreover, since the radiation is cut from the extraction half-mirror, the footprint reaching the beamline is affected from Fresnel diffraction and presents some darker zone. For these reasons the intensity of the radiation at the double slit position is not the equal in the two slits and the imbalance of the intensities must be taken into account [6]. Including this imbalance effect, the visibility is given by in Eq. 2 the simple visibility V has to be substituted by:

$$\gamma = \frac{I_1 + I_2}{2\sqrt{I_1 I_2}} \times V \tag{3}$$

where I_1 and I_2 are the intensities at each single slit of the double slit.

Several measurements were taken for different slits separations but unfortunately, for timing reasons, it was not possible to reproduce tests blocking the air flux as in the horizontal plane. For this reason for each set of measurement, only the minimum of the resulting beam sizes is considered in Fig. 10. Results still have to be improved by stabilizing the air flux.

On the other hand simulations show that the use of not monochromatic radiation strongly affect the interferogram shape for small beam sizes, for this reason the fitting algorithm has to be improved [7].

Vibration in the Optical Path

Small displacement in the mirror, or air turbulence along the optical path may change wavefront direction, which in turn produce deformation in the interferograms.

We estimate these effects by studying the displacement of the interferogram centroid during consecutive data acquisitions. The CCD exposure time is fixed to 15 ms. If the light wavefront is moving during the exposure time, several interferograms are superimposed and may cause the increasing of the visibility. Comparing standard deviation of the average position of the centroid with respect to the oscillation period

ISBN 978-3-95450-141-0

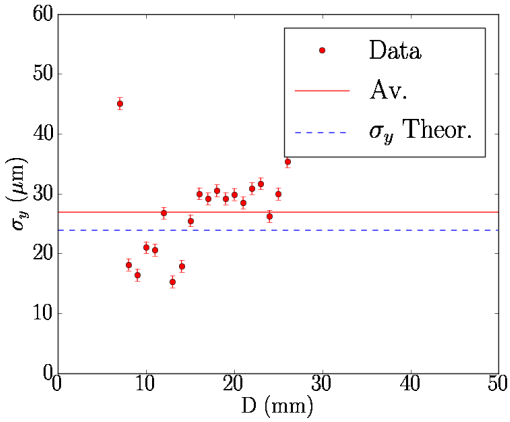

Figure 10: Vertical beam size as a function of the slit separation. The average beam size measurement is 26.9 µm, 15% larger with respect to the expected one.

of the interferogram ($\frac{2\pi D}{\lambda f}$, from Eq. 1), it was possible to have an idea of how influent was the effect which should wash out the interferogram in both horizontal and vertical direction. Figure 11 shows the ratio between the two values at different slits separations: the centroid vibration varies between 10% and 70% of the oscillation period. In both cases the displacement is large and may cause the instability of the results observed previously.

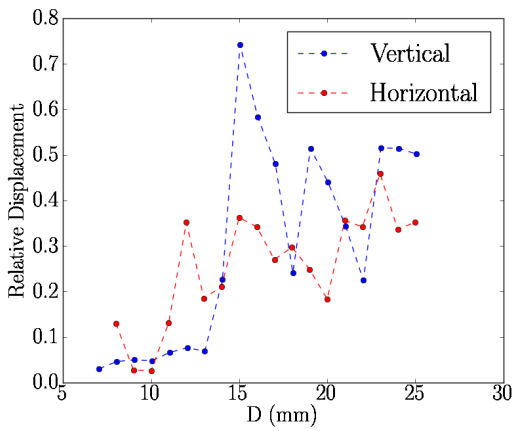

Figure 11: Ratio between the displacement in 15 ms and the period of the interferogram at different slit separation.

A further upgrade of the Xanadu beamline is taking place to prevent these effects. On top of it, we plan to use a fast CCD camera to obtain the spectrum of the interferogram vibrations to better understand their origin.

CONCLUSION

In order to obtain reliable beam size measurements using the SR interferometer, Xanadu beamline underwent to several upgrades. A better in-vacuum mirror and larger mirrors for the transport light were installed. The quality of the wavefront reaching the beamline had been carefully analyzed and strongly improved. Moreover blocking the air flux from the tunnel to the beamline allowed to obtain good and stable results for the horizontal beam size. Unfortunately this test could not be performed for the vertical beam size measurements.

In case of small beam sizes, as the one corresponding to the vertical plane, the fitting algorithm is not yet fully developed to deal with the effect of non monochromatic light. Further theoretical and practical studies will be performed in the near future.

ACKNOWLEDGMENT

We wants to thanks J. Nicolas, M. Llonch J. Ladrera, E. Pellegrin, M. Gonzalez (ALBA-CELLS), J. Pasquaud (ESRF) and all the technical staff of ALBA for their valuable help. This project is funded by the European Union within the oPAC network under contract PITN-GA-2011-289485.

APPENDIX

When the Xanadu beamline was upgraded the old in-vacuum mirror was extracted and a crystalline growth was observed on the surface. Experiments were performed together with the ALBA Experiments group to understand the nature of the growth. Results from a Raman scattering experiment shows that the growth is compatible with a nano-crystalline carbon-like-diamond structure. The results are show in Fig. 12 together with results published in literature. The peak at 1332 cm^{-1} is typical of the diamond and the one present at 1550 cm^{-1} is typical of carbon. The total structure is comparable with the footprint of nano-crystalline carbon-like-diamond. Further studies will be performed to understand the nature of the growth and prevent it if possible.

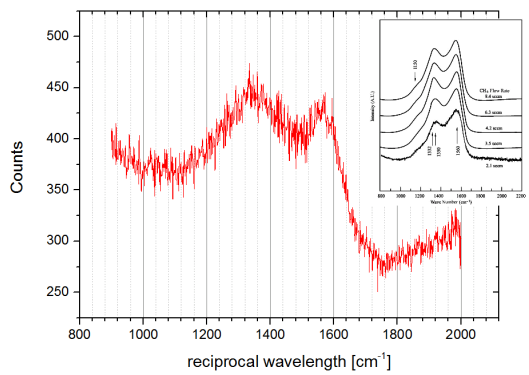

Figure 12: Raman spectrum of the old Xanadu mirror (in red) and spectra taken from the literature (inserted) [8].

REFERENCES

[1] F. Perez, "First Year Operation of the ALBA Synchrotron Light Source", IPAC2013, Shanghai, June 2013, MOPEA055 (2013)

[2] U. Iriso, "Beam size and emittance measurements using the ALBA Pinhole", AAD-SR-DI-PINH-01.

ISBN 978-3-95450-141-0

[3] T. Mitsuhashi, "Measurement of small transverse beam size using interferometry", DIPAC'2001, Grenoble, May 2001, IT06 (2001)

[4] U. Iriso, L. Torino and T. Mitsuhashi, "First Transverse Beam Size Measurements Using the Interferometry at ALBA", IBIC2013, Oxford, September 2013, MOPF01 (2013)

[5] T. Mitsuhashi. "SR Monitor – Special topics", BIW2012, Newport News, April 2012, TUAP02 (2012)

[6] M.J. Boland, T. Mitsuhashi. and K.P. Wootton "intensity imbalance optical interferometer beam size monitor", IBIC2012, Tsukuba, September 2012, WECC03 (2012)

[7] A. Arinaga et al. "KEKB beam instrumentation systems", Nuclear Instruments and Methods in Physics Research A 499 (2003) 100–137

[8] Z.L. Wang, Y. Liu and Z. Zhang "Handbook of Nanophase and Nanostructured Materials", (Kluwer Academic PublishersPlenum Publishers, 2003)

ISBN 978-3-95450-141-0